# Anomalous Quantum-Confined Stark Effects in Stacked InAs/GaAs Self-Assembled Quantum Dots

Weidong Sheng and Jean-Pierre Leburton

*Beckman Institute for Advanced Science and Technology and Department of Electrical and Computer Engineering, University of Illinois at Urbana-Champaign, Urbana, Illinois 61801*

(Received 12 June 2001; published 9 April 2002)

Vertically stacked and coupled InAs/GaAs self-assembled quantum dots (SADs) are predicted to exhibit strong hole localization even with vanishing separation between the dots, and a nonparabolic dependence of the interband transition energy on the electric field, which is not encountered in single SAD structures. Our study based on an eight-band strain-dependent $\mathbf{k} \cdot \mathbf{p}$ Hamiltonian indicates that this anomalous quantum confined Stark effect is caused by the three-dimensional strain field distribution which influences drastically the hole states in the stacked SAD structures.

DOI: 10.1103/PhysRevLett.88.167401 PACS numbers: 78.67.Hc, 71.70.Fk, 73.21.La

Zero-dimensional semiconductor structures, such as InAs/GaAs self-assembled quantum dots (SADs) [1] have attracted considerable attention because of the new physics [2–4] of a few electron systems and potential applications in optoelectronics [5]. A recent experiment on Stark effect spectroscopy in SADs [6] has demonstrated the existence of an inverted electron-hole alignment due to the presence of gallium diffusion in InAs SADs and has established a relation between the Stark shift and the vertical electron-hole separation.

The theoretical interpretation of these experimental results is based on the assumption that the applied electric field can be treated by the second-order perturbation theory, which results in a quadratical dependence of the transition energy on the applied electric field [7],

$$E(F) = E(0) + pF + \beta F^2, \tag{1}$$

where $p$ is the built-in dipole moment and $\beta$ measures the polarization of the electron and hole states, i.e., the quantum confined Stark effect (QCSE). While this relation is well satisfied in many quantum systems including single SADs [7] and quantum well structures [8,9], we show in this work that it is not valid for vertically coupled SAD structures [10] where the QCSE deviates significantly from its quadratic dependence on the electric field. The reason for this anomalous QCSE is due to the three-dimensional (3D) strain field distribution in the dots, and in the coupling region, which leads to the localization of hole states in the respective SADs, even with vanishing separation between the dots at zero electric field. The existence of this effect is important for basic condensed matter physics because it cannot be inferred from a simple superposition of the electronic properties of single SADs. It is also promising for applications in optoelectronics because interband transition energies can be significantly modulated by electric fields in quantum dot lasers and other photonic devices.

The insets in Fig. 1 show schematically a single SAD structure and a system of two vertically coupled SADs that are truncated pyramids separated by a GaAs barrier of 1.8 nm, with identical base $17.4 \times 17.4$ nm$^2$ and individual height 3.6 nm. A positive electric field $F$ is directed from the top to the bottom of the structures.

Figure 1 shows the calculated ground state transition energies for the single dot and for the stacked structure, as functions of electric fields. The electron and hole states of the system are obtained from the Schrödinger equation in the framework of the envelop function formalism [11],

$$(\mathbf{H}_{k\cdot p} + |e|Fz)\phi = E\phi\,. \tag{2}$$

Here $\phi = (\phi_1, \phi_2, \ldots, \phi_8)$ is the envelop eigenvector and $\mathbf{H}_{k\cdot p}$ is the $\mathbf{k} \cdot \mathbf{p}$ eight-band Hamiltonian which includes the effect of strain and piezoelectricity [12,13]. The strain tensor is calculated by using continuum elasticity theory and minimizing the strain energy on a grid of $150 \times 150 \times 150$ sites. The Hamiltonian is then solved, excluding irrelevant GaAs sites, on a reduced grid by the Lanczos algorithm. All the material parameters are taken from Ref. [13]. This approach has been shown to be reliable,

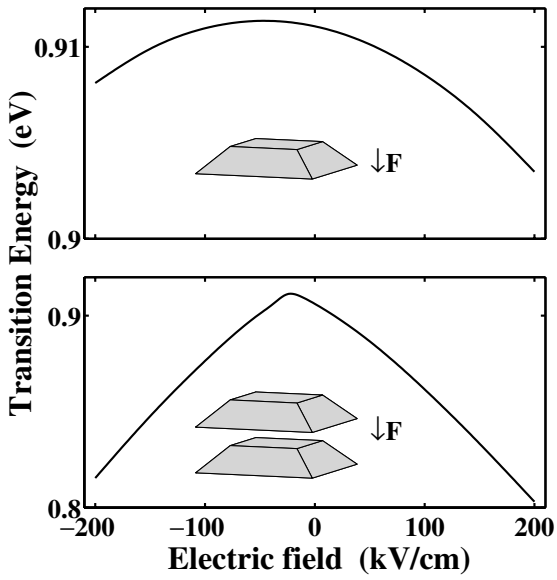


FIG. 1. Ground state transition energies as functions of vertical electric fields for single dot (top) and stacked double dots (bottom). The insets show the dot systems schematically.

  

especially in the investigation of the inverted electron-hole alignment in SAD structures [14].

The single dot exhibits a nearly perfect quadratical dependence on the electric field which is referred to the conventional QCSE and has been observed in many other types of quantum structures [7–9]. The maximum transition energy occurs at $F \approx -50$ kV/cm because this homogeneous InAs SAD has a positive electron-hole alignment, i.e., the hole is at the bottom of the dot for zero electric field. The stacked structure shows piecewisely quasilinear dependence, with a turning point at a smaller negative electric field $F \approx -22$ kV/cm. The lower panel of Fig. 1 shows that this discrepancy from the conventional QCSE occurs over the whole range of electric field, i.e., for $200 \leq F \leq 200$ kV/cm. In addition, the stacked structure exhibits a Stark shift of 1 order of magnitude stronger than the single dot. We also notice that the maximum transition energy for both systems is roughly identical, because in the stacked structure, despite the downshift of the electron states due to tunnel coupling, the hole states are characterized by an up-shift in energy due to the strain distribution (see Fig. 2). Similar simulations have been performed for stacked structures with different sizes, with or without wetting layers, and with different separations. It was found that the anomalous behavior persists until the two dots are separated by a distance larger than 40 Å for which they are quantum mechanically decoupled, in agreement with Fonseca *et al.* [12].

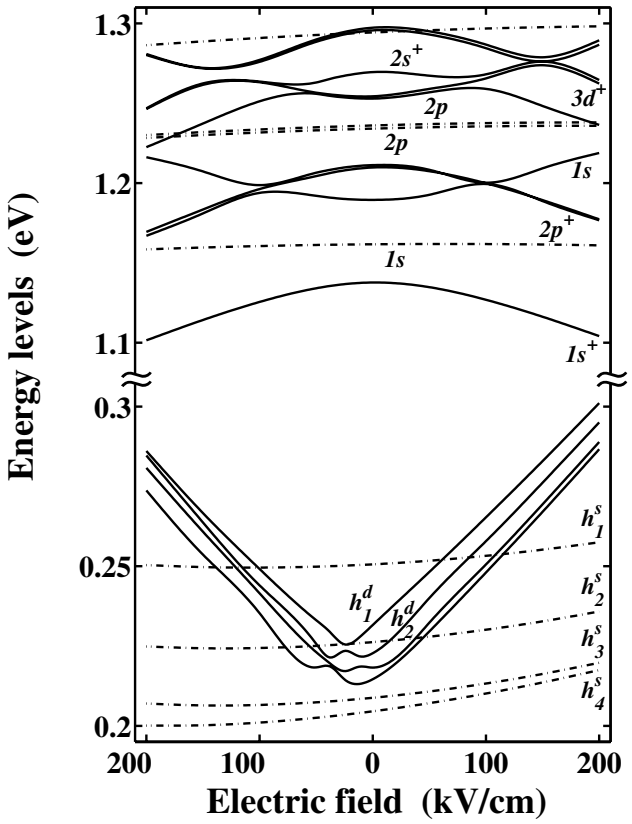


FIG. 2. Energy levels of stacked double dots, as a function of the electric field. The dash-dotted lines are for the single dot of the same size.

Figure 2 shows the energy levels of the stacked structure, for both electrons and holes, as a function of electric fields. All the energies are given in reference to the top of the valence bands of GaAs. In order to show the fine structure of the hole spectra near zero electric field, we use an energy scale twice as small as for electrons. It is clearly seen that, due to the coupling between the stacked structures, the double dot system exhibits a much richer structure in its energy spectrum.

In the conduction band, the energy spectrum of the single dot shows the ground $1s$ state, the two nearly degenerate excited $2p$ states, and the $3d$-like state with weak sensitivity to the electric field. The coupled dot system results in bonding and antibonding states originating from these states, that in the absence of electric field, are identified as $1s^+, 1s^-, 2p^+, 2p^-, 2s^+, 3d^+, \ldots$, where $+$ $(-)$ denotes bonding (antibonding) states. Except for the ground state, all the excited states are seen to have crossings or anticrossings with other states, which reorders the states at high fields. In the valence bands of the single dot, the four hole levels ($h^s_1$, $h^s_2$, $h^s_3$, and $h^s_4$) are seen to show quadratical dependence on the electric field.

The most dramatic feature in the valence bands of the stacked structure is the quasilinear dependence of the hole levels on the electric field for intermediate and strong field intensities, especially the ground hole state $h^d_1$. In addition, we could not find any bonding or antibonding hole states for these structures as the ground hole state $h^d_1$ and first excited state $h^d_2$ are localized in the bottom dot and the top one, respectively. However, at small electric fields, the hole levels experience small fluctuations due to mutual anticrossings. It is also noticed that the magnitude of the Stark shift for holes in the stacked structure is significantly larger than in the single dot, which is responsible for the large shift in the transition energy shown in Fig. 1.

The main reason for the hole states to behave so differently in the stacked structure than in the single dot is traced in the 3D strain field distribution. Figure 3(a) shows the profiles and the corresponding contour plots (insets) for the hydrostatic ($H$) and the biaxial ($B$) components of the strain field, which are defined as

$$\begin{aligned} H &= \epsilon_{xx} + \epsilon_{yy} + \epsilon_{zz}\,, \\ B^2 &= (\epsilon_{xx} - \epsilon_{yy})^2 + (\epsilon_{yy} - \epsilon_{zz})^2 + (\epsilon_{zz} - \epsilon_{xx})^2. \end{aligned} \tag{3}$$

Here, we show only the absolute value of the biaxial strain $|B|$ [3], which directly influences the valence band edges. The diagrams of the conduction $U_c$ and valence band edges $U_v$ through the central axis along the growth direction are given by [15]

$$\begin{aligned} U_c &= \Delta E_c + a_c H\,, \\ U_v^{\pm} &= \Delta E_v - a_v H \pm b|B|/\sqrt{2}\,, \end{aligned} \tag{4}$$

where $\Delta E_c$ ($\Delta E_v$) is the unstrained conduction (valence) band offset, $a_c$ ($a_v$) is the conduction (valence) band

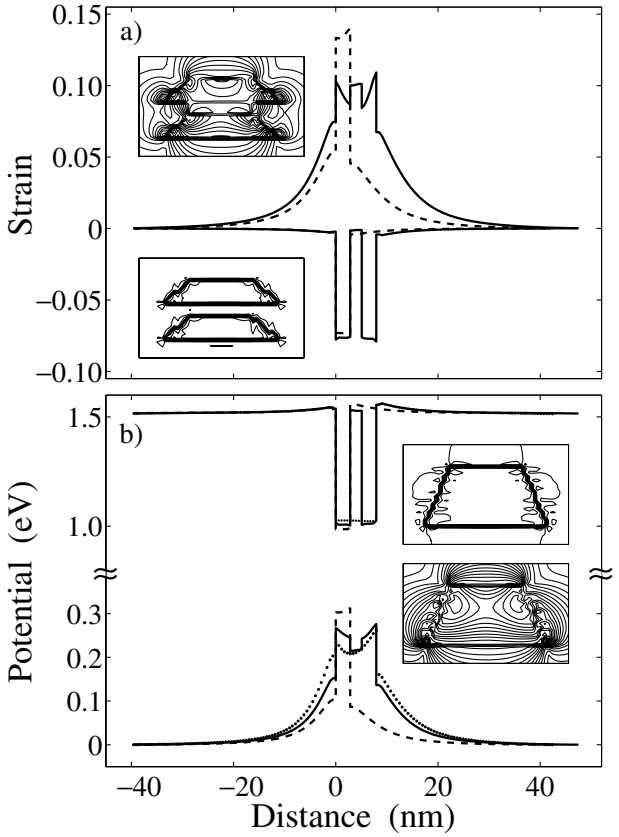


FIG. 3. (a) Biaxial (upper curve) and hydrostatic (lower curve) components of the strain field in the single (dashed lines) and stacked (solid lines) SAD structures through the center of the dots along the growth direction ($z$). The zero on the horizontal axis is fixed at the top of the upper dot. (b) Band diagrams for the single (dashed lines) and stacked (solid lines) SAD structures, and a thick single SAD structure (dotted lines). Inset: Contour plots of the two strain components in the stacked structure (left panels) and in the thick single SAD structure (right panels).

hydrostatic deformation potential parameter, and $b$ is the valence band deformation potential parameter. Under strain, the degenerate heavy and light hole valence bands split into two ($\pm$) mixed bands [16], each containing the components of both heavy holes and light holes. Figure 3(b) shows $U_c$ and $U_v^-$ which is the lower band.

In the stacked structure, the hydrostatic strain field resides entirely inside the dots and is a little stronger than in the single dot, while it almost vanishes in the coupling region [lower curve in Fig. 3(a)]. Therefore, the coupling region is seen by electrons as a conventional tunneling barrier, which results in bonding and antibonding states (Fig. 2). The biaxial strain field is, however, seen very differently in the stacked structure from that in the single dot [upper curve in Fig. 3(a)]. First, it is smaller than in the single dot, leading to hole levels with higher energies in the stacked system (see Fig. 1). Second, unlike the hydrostatic strain, the biaxial strain retains a substantial value in the coupling region in the stacked system [top inset of Fig. 3(a)], which noticeably reduces the barrier height in the valence bands. Third, the biaxial strain profile in the stacked structure is inverted in the upper dot compared to the lower one although symmetric with respect to a median plane between the dots.

The most important point is that the biaxial strain defines two triangular confining potentials in each dot of the stacked structure, while in the single dot the valence band edge profile exhibits a much smoother slope [see Fig. 3(b)]. It is seen that the strain-induced triangular potential is inverted with respect to the base in the two dots: In the bottom dot, the valence band edge is higher at the base than at the top, while it is opposite in the top dot. Therefore, the favorable combination of the lower strain-induced potential and the wider base result in a weaker hole confinement in the bottom dot than in the top dot, thereby localizing the hole ground state in the lower dot.

For comparison, we also show the band edge profiles of a single large, although unrealistic dot spreading from the bottom of the lower dot to the top of the upper dot, with the respective hydrostatic and biaxial contour plots. The conduction band edge is relatively flat, but the valence band exhibits similar inverted triangular wells, although smoother and shallower than in the double structure, especially for the top dot. This situation is the result of the weak biaxial strain in the center of the dot visible in the lower contour plot panel of Fig. 3(b).

The hole localization in the double dots is illustrated in the middle panel of Fig. 4(a) where we plot the probability density isosurfaces of ground electron and hole states at different electric fields. In contrast, the ground electron state is the bonding $1s^+$ state extending quasiequally in both dots and in the coupling region. Under positive electric field, the ground electron state in the right panel of Fig. 4(a) becomes a $1s$-like state progressively localized in the upper dot. However, the ground hole state behaves very differently. Because it is localized entirely inside the

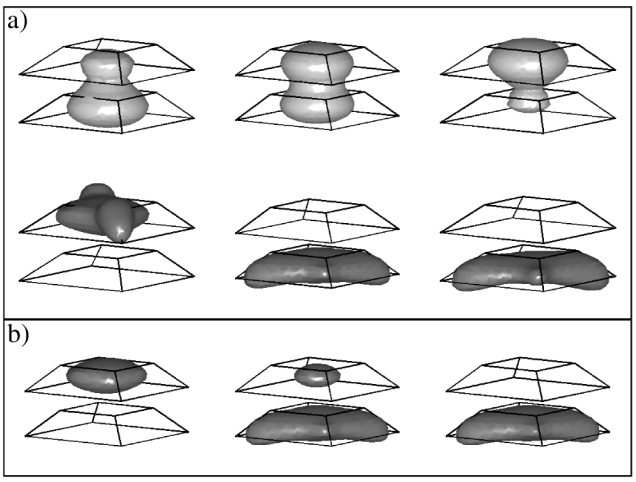


FIG. 4. Probability density isosurfaces (70%) of ground states of electron (top panel) and hole (two bottom panels) at different electric fields. From left to right, the electric field is (a) $F = -50$, 0, and $+50$ kV/cm; (b) $F = -21.8$, $-21.6$, and $-21.4$ kV/cm, respectively.

triangular potential, the hole energy level changes approximately by the same amount as the potential drop between the two dots, resulting in a linear dependence in the external electric field. Although the overlap between electron and hole states decreases, oscillator strength calculation shows that the ground state transition remains significant up to $\pm 100$ kV/cm. Hence, while the weak displacement of the $1s^+$ electron state is the result of the strong quantum mechanical coupling between the two dots (Fig. 2), the large variation of the hole states is the result of their localization in a single dot. Our model shows this localization persists even at vanishing interdot separation and is the cause of the quasilinear dependence of the ground state transition energy as shown in Fig. 1.

Figure 4(b) illustrates the transition of the ground hole state from the bottom dot to the top one occurring at a small negative electric field $F = -21.6$ kV/cm. As the biaxial strain field has a different distribution in the respective dots, the hole states exhibit different probability density profiles when localizing in different dots. In Fig. 2, this transition is seen as an anticrossing between the ground hole state and the first excited state, which also accounts for the anomalous QCSE.

Although the anomalous QCSE invalidates Eq. (1) over the whole range of the electric field, one can write two separate equations that describe the dependence of the transition energy on the electric field for the stacked structure, except for the electric fields at which anticrossings occur.

$$E^+(F) = E(0) + p^+F + \beta^+F^2, \quad F > -21.4\ \text{kV/cm},$$
$$E^-(F) = E' + p^-F + \beta^-F^2, \quad F < -21.8\ \text{kV/cm}, \tag{5}$$

where $E'$ is a fitting parameter.

The QCSE coefficient is defined by $\beta = \beta_e - \beta_h$, where $\beta_e$ ($\beta_h$) can be related to the oscillator strength of optical intraband transitions in conduction (valence) bands [7,17]. For instance, $\beta_e$ is given by

$$\beta_e = -\frac{\hbar^2}{2m_0} \sum_{n>1} f_{1\to n}/(E_n - E_1)^2, \tag{6}$$

where $m_0$ is the bare electron mass and $f_{1\to n}$ is the oscillator strength for the intraband transition from the ground state to the $n$th state, with polarization along the $z$ direction. $\beta_h$ has a similar expression. Single SAD structures have very weak $z$-polarized intraband transitions [18]; therefore, both $\beta_e$ and $\beta_h$ are small. In the stacked structure, the strengths of the $z$-polarized intraband transitions in the valence bands are similar to those in the single dot. However, in the conduction band of the stacked structure, there are several strong intraband transitions, especially the $1s^+ \to 1s^-$ transition [18]. This results in a larger $\beta_e$ than in single dots and explains the magnitude of the QCSE coefficients in both branches ($\beta^\pm/|e|^2 \approx -80\ \text{nm}^2/\text{eV}$) which are 6 times larger than in single dots, and are responsible for the strong "bowing" of the Stark shift at low field, i.e., $-50\ \text{kV/cm} \le F \le 0$ (Fig. 1).

Experimental evidence of this anomalous QCSE could be performed by measuring photocurrent in a $p$-$i$-$n$ structure similar to the one used by Fry and co-workers in their investigation of electron-hole alignment in single SAD [6]. The measurement may require a higher detecting resolution than in single SADs owing to the splitting of the ground state transition and the electron and hole localization in different dots with applied electric fields. These effects result in weaker oscillator strengths, decreasing with electric fields. However, as the anomalous QCSE already occurs at low fields, measurements at high fields may not be necessary. Let us point out that the observation of the anticrossing structures at low fields also requires reduced inhomogeneous broadening of the photocurrent peaks, which should be achieved with uniform dots or by sampling only a few of them.

In conclusion, we have shown that vertically stacked InAs/GaAs self-assembled quantum dots exhibit, in addition to a larger Stark shift than single dots, a strong nonparabolic dependence of interband transition energy on the electric field, due to the 3D distribution of the biaxial strain field. While it is well known that In-Ga interdiffusion in the dot may soften the strain distribution in and around the dot, we may expect this anomalous QCSE to persist as long as the hole states remain localized in their respective dots. The potential profile of the large dot shown in the Fig. 3(b) inset is indicative in this respect.

This work is supported by Army Research Office Grant No. DAAD 10-99-10129 and National Computational Science Alliance Grant No. ECS000002N.

[1] D. Bimberg *et al., Quantum Dot Heterostructures* (John Wiley & Sons, Chichester, U.K., New York, 1998); see also L. Jacak *et al., Quantum Dots* (Springer, Berlin, 1998).
[2] Y. Ebiko *et al.,* Phys. Rev. Lett. **80**, 2650 (1998).
[3] O. Stier *et al.,* Phys. Rev. B **59**, 5688 (1999).
[4] I. Kegel *et al.,* Phys. Rev. Lett. **85**, 1694 (2000).
[5] D. L. Huffaker *et al.,* Appl. Phys. Lett. **73**, 2564 (1998).
[6] P. W. Fry *et al.,* Phys. Rev. Lett. **84**, 733 (2000).
[7] J. A. Barker *et al.,* Phys. Rev. B **61**, 13 840 (2000).
[8] E. E. Mendez *et al.,* Physica (Amsterdam) **117B**, 711 (1983).
[9] M.-E. Pistol *et al.,* Phys. Rev. B **50**, 11 738 (1994).
[10] H. Eisele *et al.,* Appl. Phys. Lett. **75**, 106 (1999).
[11] T. B. Bahder, Phys. Rev. B **41**, 11 992 (1990).
[12] L. R. C. Fonseca *et al.,* Phys. Rev. B **58**, 9955 (1998).
[13] C. Pryor, Phys. Rev. B **57**, 7190 (1998).
[14] W. Sheng and J.-P. Leburton, Phys. Rev. B **63**, 161301(R) (2001).
[15] T. B. Bahder, Phys. Rev. B **45**, 1629 (1992).
[16] C. Pryor, Phys. Rev. Lett. **80**, 3579 (1998).
[17] W. Sheng and J.-P. Leburton (unpublished).
[18] W. Sheng and J.-P. Leburton, Appl. Phys. Lett. **78**, 1258 (2001).